

## Supplementary Information for

### **Voltage-modulated van der Waals interaction in single-molecule junctions**

Yujing Wei<sup>a</sup>, Liang Li<sup>a</sup>, Julia E. Greenwald<sup>a</sup>, Latha Venkataraman<sup>\*a,b</sup>

<sup>a</sup>Department of Chemistry, Columbia University, New York, New York 10027, United States

<sup>b</sup>Department of Applied Physics and Applied Mathematics, Columbia University, New York, New York 10027, United States

Email: [lv2117@columbia.edu](mailto:lv2117@columbia.edu)

#### **Table of Contents**

- 1. Determination of experimental parameters.**
- 2. Eliminating linear dependence of conductance and modulation amplitude with modulation response.**
- 3. Second harmonic peaks in FFT for molecular junction.**
- 4.  $\pi$ -stacking interactions.**
- 5. Polarizability and dipole moment of molecular orbitals.**
- 6. References**

## 1. Determination of experimental parameters

We obtain  $\omega_p$  and  $\omega_v$  (Eq. 1 and 2 in the main text) by applying a voltage to the piezo and junction respectively, as a function of time, as a sine wave at the desired frequency. The conductance FFT spectrum of a modulated trace (Figure 1B in the main text), showing clean peaks at  $\omega_p$  and  $\omega_v$  confirms that the actual measured frequency is the same as the applied frequency. The junction voltage is measured through a data acquisition system (NI PXI-4461), and we determine  $V_1$  to be 26 mV in our experiments.

### *Calibration of piezoelectric amplitude $x_1$ using tunnel junctions*

The procedure for amplitude calibration involved a push-pull experiment<sup>1</sup> where, upon rupture of the junction, the electrodes are pushed towards each other at constant speed. Figure S1A shows this procedure for one trace. During the “push” region, the measured conductance can be observed to increase from the instrument noise value to the Au-Au contact value of  $\geq 1G_0$ . The conductance follows an exponential increase with decreasing length and a decay constant  $\beta$  (main text Eq. 1). Note that due to relaxation of the gold electrodes during separation (“snapback”)<sup>1-3</sup>, we cannot fit the “pull” segment of the trace with this equation. We measure a  $\beta$  of  $0.91 \text{ \AA}^{-1}$  based on the slope of a Gaussian fit of the 2D conductance-displacement histogram (Figure S1B) for a clean gold measurement in air, which is comparable to the value found for tunnel junctions in literature<sup>4,5</sup>.

We then use the method presented in the main text (main text Eq. 5) to obtain  $b$  for the Au-Au tunnel junction. Since for a tunnel junction  $\beta = b$  (Eq. 3 in the main text), we can calibrate the piezo amplitude and obtain the value of  $x_1$ , the modulation amplitude of the piezoelectric actuator. In Figure S1C, we take the normalized FFT magnitude of the conductance at the piezo modulation frequency,  $\omega_p$ , and determine value of  $\xi = G_{\omega_p}/G_{\text{avg}}$  is 1.05, which from Eq. 5 in the main text,

suggests an amplitude of  $x_1 = \frac{\xi}{b} = \frac{\xi}{\beta} = \frac{1.05}{0.907} \approx 1.2 \text{ \AA}$ .

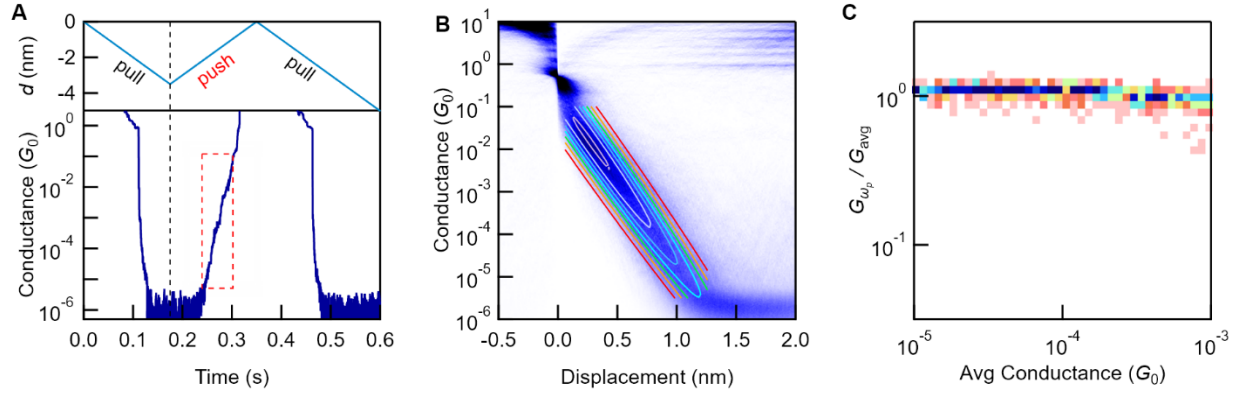


Figure S1. (A) Push-pull measurement for a single trace. Top panel: programmed piezo position as a function of time, with zero displacement ( $d=0$ ) at the start of the trace when the electrodes are in contact with a conductance greater than  $5G_0$ . Bottom panel: conductance as a function of time. (B) 2D histogram of displacement against conductance of a Au tunnel junctions during the push region of the measurement, of over 15 000 acquired contiguously, aligned at  $0.5G_0$ . (C) 2D histogram of normalized FFT magnitude at the piezo modulation frequency against the average conductance during the hold, using the procedure in the main text.

#### Delay in piezo response to the piezo voltage input

The delay in piezo response is small compared to the length of a modulation cycle. This delay compared to the length of one cycle is around 15 degrees on average, as shown in Figure S2. For a sinusoidal modulation, the phase of the conductance FFT during the modulation without delay is expected to be 90 degrees, and we measure on average 105 degrees.

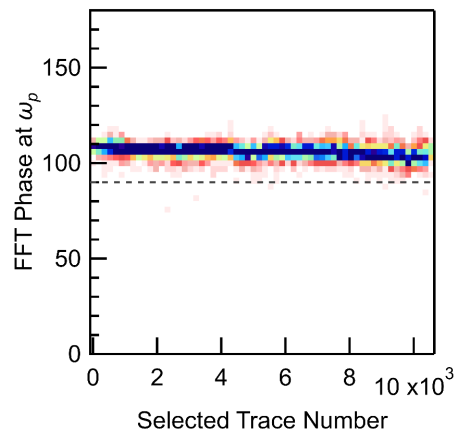
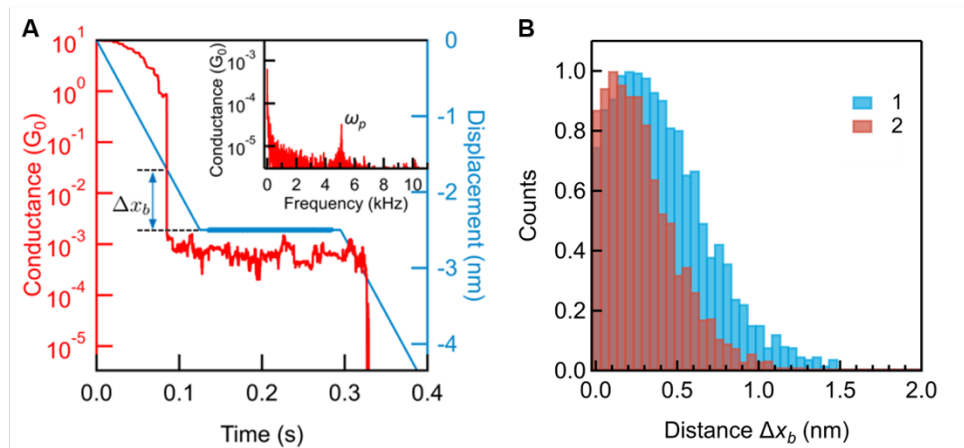


Figure S2. 2D histogram of the phase of the FFT of the conductance of molecular junctions during modulation at  $\omega_p$ , of over 10000 traces of molecule 2, selected according to the criterion described in the methods section in the main text. The dashed line indicates the expected phase if no delay is experienced in the measurement.

The phase being consistent throughout the measurement indicates that the delay is constant and should not affect the conductance FFT magnitude, which is what we base our results on in the main work.

### *Estimation of mean electrode separation $x_0$ for the molecular junctions*

Due to the snapback mentioned above,  $x_0$  (main text Eq. 1) cannot be measured exactly for each trace. However, an estimate can be obtained from the difference in electrode displacement between when a gold atomic contact is formed at a conductance of  $G_0$  to when the molecular junction is formed ( $\Delta x_b$  in Figure S3A). In practice,  $x_0 > \Delta x_b$  due to the additional snapback (Au electrode relaxation) upon breaking the Au-Au contact. As a comparison, Figure S3B shows  $\Delta x_b$  of molecules **1** and **2** in the main text. This result confirms that the junctions for **1** are in general longer than for **2** by a small amount (on the order of angstroms), which is expected given the geometries of these molecules. This also rules out the possibility of **2** forming  $\pi$ -stacked dimers in the junction, as these are expected to have a comparably larger  $x_0$ , and hence  $\Delta x_b$  than the monomer junction (See SI section 4 for an example).



*Figure S3. (A) Conductance trace (red) of a single molecular junction against the electrode displacement, where the molecular junction is modulated in a similar fashion to Figure 1B in the main text. Indicated on the diagram is  $\Delta x_b$ , the difference in displacement between breaking the Au-Au atom contact at  $G_0$  to where we hold the electrode separation at  $x_0$  and apply a modulation. In the absence of snapback,  $\Delta x_b = x_0$ . The inset shows the conductance FFT spectrum of the trace during the hold. (B) Normalized histogram of  $\Delta x_b$  for molecules **1** and **2** in the main text (see Figure 2A for chemical structures) over thousands of traces, at 500 mV (average) applied bias.*

## 2. Eliminating linear dependence of conductance and amplitude with modulation response.

Figure S4A and S4B show that normalizing  $G_{\omega_p}$  by  $G_{\text{avg}}$  removes the correlation of  $G_{\omega_p}$  with conductance, and hence  $\xi = bx_1 = G_{\omega_p}/G_{\text{avg}}$  can be used to compare molecules and junctions with different conductances (although not to be confused with the exponential decay constant for tunnel junctions<sup>4</sup> or molecular series<sup>6-11</sup>). Furthermore,  $b = \frac{1}{x_1} G_{\omega_p}/G_{\text{avg}}$  (main text Eq 5) is independent of  $x_1$ , the displacement modulation amplitude, at least in our regime of small modulation amplitudes, as shown in Figure S4C and S4D.

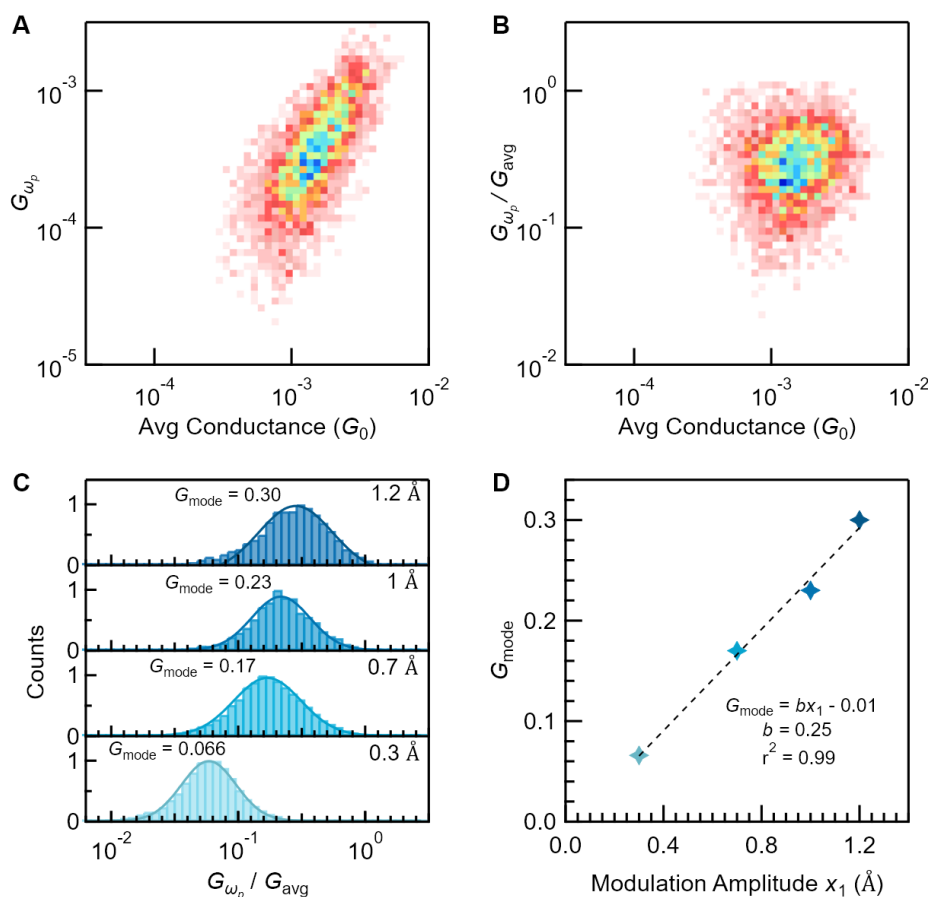


Figure S4. (A) 2D histograms of  $G_{\omega_p}$  against  $G_{\text{avg}}$  for molecule **1** measured at an average bias of 500 mV with a voltage modulation amplitude of 26 mV and displacement modulation amplitude of 1.2 Å. (B) Data in (A) normalized by the average conductance. (C) 1D histogram of conductance-normalized FFT magnitude  $G_{\omega_p}/G_{\text{avg}}$  at different distance modulation amplitudes as indicated in each panel for molecule **1**. Gaussian fits are drawn to guide the eye.  $G_{\text{mode}}$  is the most probable value of  $G_{\omega_p}/G_{\text{avg}}$ . (D)  $G_{\text{mode}}$  displayed for each modulation amplitude in (C) against modulation amplitude. The slope of the linear fit is  $b$  (effective decay constant as described in the main text).

### 3. Second harmonic peaks in FFT for molecular junction.

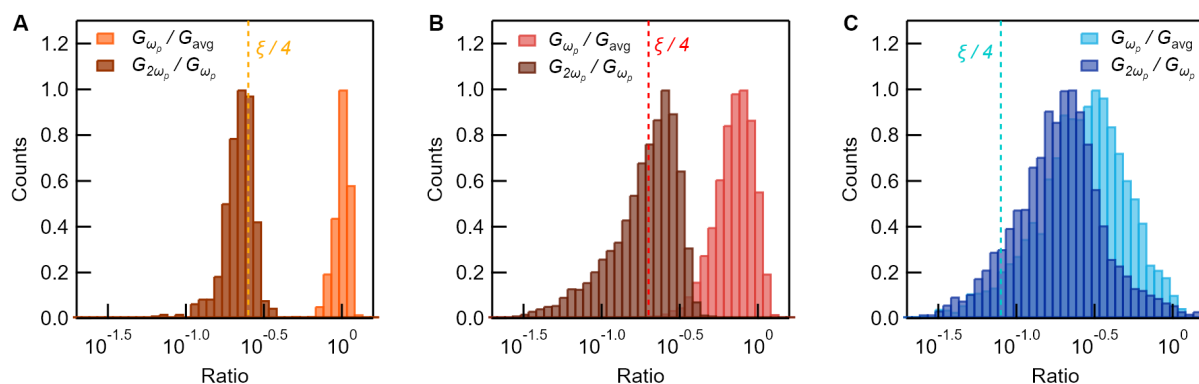


Figure S5. Histograms of the ratio of first to zeroth harmonic and second to first harmonic of (A) Au tunnel junctions (B) Molecule 2 and (C) Molecule 1. The dashed line indicates where peak of the histogram for ratio of the second to first harmonic would lie if the molecular junction followed an exponential decay model described by Eq. 3 in the main text.

### 4. $\pi$ -stacking interactions.

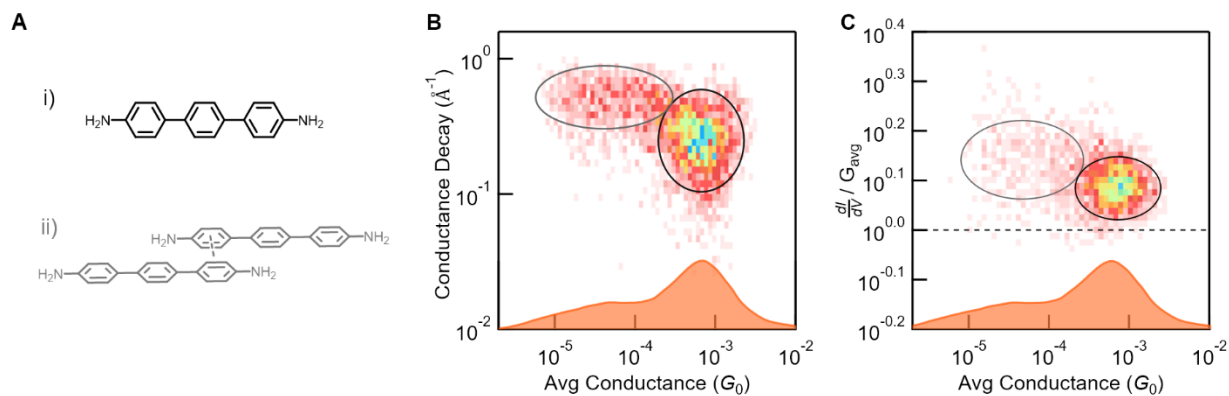


Figure S6. (A) Schematic representation of i) the 4,4''-diamino-p-terphenyl high-conducting junction, and ii) 4,4''-diamino-p-terphenyl low-conducting  $\pi$ -stacked junction, as described in Magyarkuti et al.<sup>12</sup> (B) 2D histogram of the effective exponential conductance decay against average conductance, and (C) 2D histogram of the normalized  $dI/dV$  against average conductance, of the 4,4''-diamino-p-terphenyl molecule. The overlay is a 1D histogram of the conductance during the hold.

As a proof of concept, this modulation method can also distinguish junctions formed by other weak interactions such as those by  $\pi$ -stacking. As has been previously shown<sup>12</sup>, the 4,4''-diamino-p-terphenyl molecule forms both a high-conducting and low-conducting junction, indicative of a single-molecule and  $\pi$ -stacked junction, respectively. We show in Figure S6 that the high-

conducting and low-conducting junctions are distinguishable using the method we present in the manuscript (see Figure 1 and Figure 2). Interestingly, the differential conductance for the  $\pi$ -stacked junctions is broadly distributed.

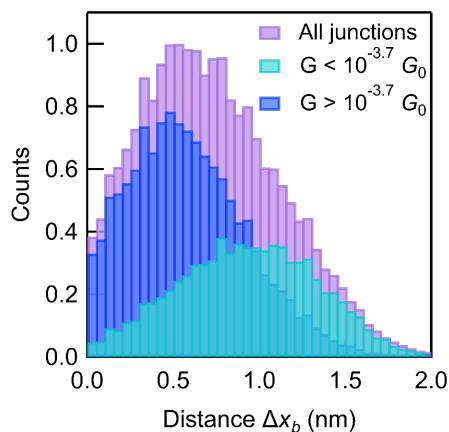


Figure S7. Measure of electrode separation  $\Delta x_b$  (see SI section 1 for details) of the high-conducting (monomer) and low conducting (dimer) junctions. The high-low conductance cutoff of  $10^{-3.7} G_0$  was determined by using the intersection of a double Gaussian fit of the conductance histogram of the 4,4''-diamino-*p*-terphenyl molecule.

### 5. Polarizability and dipole moment of molecular orbitals.

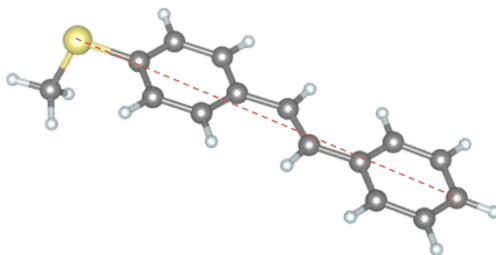


Figure S8. Model of **2** without electrodes (light blue: H, grey: C, light yellow: S). The red line indicates the  $S \rightarrow C$  direction of the added external electric field vector in the calculation.

Using the FHI-aims package<sup>13</sup>, we relax the geometry of molecule **2** without electrodes and calculate the dipole moment and polarizability with and without a field. The dipole moment of molecule **2** is 1.88 Debye without an external field and 2.76 D (or  $0.575 e\text{\AA}$ ) in a 500 mV/nm field pointing along the dipole. This dipole moment is not large enough to cause the molecule to reorient in the field since the potential energy under a 500 mV/nm field is:

$$|U| = |\vec{p} \cdot \vec{E}| = 0.575 \text{ eÅ} \cdot \frac{0.500V}{10\text{Å}} = 0.029eV$$

which is close to  $kT$  at room temperature, and critically, much less than the Au-SMe bond energy, which is closer to 0.5 eV.<sup>14</sup> Thus, the electric field itself is unlikely to change the molecular orientation in the junction. The mean polarizability changes from 252.34 a<sub>0</sub><sup>3</sup> to 252.60 a<sub>0</sub><sup>3</sup> upon addition of the 500 mV/nm field. This is not a significant increase indicating that the electronic structure of the molecule is not changed significantly in the field.

## 6. References.

- (1) Fu, T.; Frommer, K.; Nuckolls, C.; Venkataraman, L., Single-Molecule Junction Formation in Break-Junction Measurements, *J. Phys. Chem. Lett.*, **2021**, 12, 10802-10807.
- (2) Quek, S. Y.; Kamenetska, M.; Steigerwald, M. L.; Choi, H. J.; Louie, S. G.; Hybertsen, M. S.; Neaton, J. B.; Venkataraman, L., Mechanically Controlled Binary Conductance Switching of a Single-Molecule Junction, *Nat. Nanotechnol.*, **2009**, 4, 230-234.
- (3) Hong, W.; Manrique, D. Z.; Moreno-García, P.; Gulcur, M.; Mishchenko, A.; Lambert, C. J.; Bryce, M. R.; Wandlowski, T., Single Molecular Conductance of Tolanes: Experimental and Theoretical Study on the Junction Evolution Dependent on the Anchoring Group, *J. Am. Chem. Soc.*, **2011**, 134, 2292-2304.
- (4) Scheer, E., *Molecular Electronics: An Introduction to Theory and Experiment*. World Scientific: 2010; Vol. 1.
- (5) Binnig, G.; Rohrer, H.; Gerber, C.; Weibel, E., Vacuum tunneling, *Physica B+C*, **1982**, 109-110, 2075-2077.
- (6) Meisner, J. S.; Kamenetska, M.; Krikorian, M.; Steigerwald, M. L.; Venkataraman, L.; Nuckolls, C., A Single-Molecule Potentiometer, *Nano Lett.*, **2011**, 11, 1575-1579.
- (7) Meisner, J. S.; Ahn, S.; Aradhya, S. V.; Krikorian, M.; Parameswaran, R.; Steigerwald, M.; Venkataraman, L.; Nuckolls, C., Importance of Direct Metal- $\pi$  Coupling in Electronic Transport Through Conjugated Single-Molecule Junctions, *J. Am. Chem. Soc.*, **2012**, 134, 20440-20445.
- (8) Gunasekaran, S.; Hernangomez-Perez, D.; Davydenko, I.; Marder, S.; Evers, F.; Venkataraman, L., Near Length-Independent Conductance in Polymethine Molecular Wires, *Nano Lett*, **2018**, 18, 6387-6391.

- (9) Garner, M. H.; Bro-Jørgensen, W.; Pedersen, P. D.; Solomon, G. C., Reverse Bond-Length Alternation in Cumulenes: Candidates for Increasing Electronic Transmission with Length, *Journal of Physical Chemistry C*, **2018**, 122, 26777-26789.
- (10) Li, L.; Gunasekaran, S.; Wei, Y.; Nuckolls, C.; Venkataraman, L., Reversed Conductance Decay of 1D Topological Insulators by Tight-Binding Analysis, *The Journal of Physical Chemistry Letters*, **2022**, 9703-9710.
- (11) Zhang, B.; Garner, M. H.; Li, L.; Campos, L. M.; Solomon, G. C.; Venkataraman, L., Destructive quantum interference in heterocyclic alkanes: the search for ultra-short molecular insulators, *Chem. Sci.*, **2021**, 12, 10299-10305.
- (12) Magyarkuti, A.; Adak, O.; Halbritter, A.; Venkataraman, L., Electronic and mechanical characteristics of stacked dimer molecular junctions, *Nanoscale*, **2018**, 10, 3362-3368.
- (13) Blum, V.; Gehrke, R.; Hanke, F.; Havu, P.; Havu, V.; Ren, X.; Reuter, K.; Scheffler, M., Ab initio molecular simulations with numeric atom-centered orbitals, *Comp. Phys. Commun.*, **2009**, 180, 2175-2196.
- (14) Park, Y. S.; Whalley, A. C.; Kamenetska, M.; Steigerwald, M. L.; Hybertsen, M. S.; Nuckolls, C.; Venkataraman, L., Contact Chemistry and Single- Molecule Conductance: A Comparison of Phosphines, Methyl Sulfides, and Amines, *J. Am. Chem. Soc.*, **2007**, 129, 15768-15769.